Stereodynamics of 2-(Diethylamino)propane and 2-(Dibenzylamino)propane. ^1H and $^{13}C\{^1H\}$ DNMR Studies. Molecular Mechanics Calculations

Jay H. Brown and C. Hackett Bushweller*

Contribution from the Department of Chemistry, University of Vermont, Burlington, Vermont 05405-0125

Received September 13, 1995[⊗]

Abstract: 2-(Diethylamino)propane (**DEAP**) and 2-(dibenzylamino)propane (**DBAP**) possess similar molecular symmetries. Interconversion among the stable equilibrium conformations occurs by inversion−rotation at the pyramidal nitrogen and by isolated rotation about carbon−nitrogen bonds. In **DEAP** and **DBAP**, the fact that stable equilibrium conformations cannot have destabilizing *syn*-1,5 interactions between methyl or phenyl groups limits the number of equilibrium conformations that will be present at concentrations high enough to be NMR detectable. The ^1H and $^{13}C\{^1H\}$ NMR spectra of **DEAP** at 100 K show two diastereomeric pairs of enantiomeric conformations. One pair of enantiomers has the isopropyl methine proton and both ethyl methyl groups gauche to the lone pair (75%). The other pair has the methine proton anti to the lone pair with the ethyl methyl groups respectively gauche and anti to the lone pair (25%). The barrier to inversion−rotation in **DEAP** ($\Delta G^{\ddagger} = 6.4$ kcal/mol) is higher than barriers to isolated rotation about carbon−nitrogen bonds ($\Delta G^{\ddagger} = 5.3-5.7$ kcal/mol). The ^1H and $^{13}C\{^1H\}$ NMR spectra of **DBAP** at 100 K show just one pair of enantiomeric conformations that have the isopropyl methine proton and both phenyl groups gauche to the lone pair. There is no evidence in the NMR spectrum at 100 K for those conformations of **DBAP** that have a phenyl group anti to the lone pair. The barrier to inversion−rotation in **DBAP** ($\Delta G^{\ddagger} = 6.4$ kcal/mol) is higher than the barrier to racemization via isolated rotation about carbon−nitrogen bonds ($\Delta G^{\ddagger} = 5.5$ kcal/mol). Molecular mechanics calculations of conformational energies are in good agreement with the observed conformational preferences.

Introduction

Exchange among the equilibrium conformations of a simple tertiary aliphatic amine occurs via isolated rotation about single bonds and via inversion at the pyramidal nitrogen.[1-3] Pyramidal inversion is a complex process that involves not only inversion at nitrogen but also concomitant rotation about carbon−nitrogen bonds.[1-4] In simple aliphatic amines, isolated rotation barriers (no inversion) about carbon−nitrogen bonds are usually substantially smaller than barriers to inversion−rotation at nitrogen.[1] Conformational preferences and isolated rotation barriers in many simple amines including methylamine,[5] dimethylamine,[5] trimethylamine,[5] ethylamine,[6] isopropylamine,[7] ethylmethylamine,[8] and dimethylethylamine[9] have been determined by Raman, infrared, or microwave spectroscopy and computed using molecular orbital theory. Inversion barriers have been measured in ammonia,[10] methylamine,[5a,11] dimethylamine,[5c] and trimethylamine.[12]

Dynamic NMR (DNMR) studies[13] complemented by molecular mechanics calculations[14] have been useful in elucidating the stereodynamics of progressively more sterically encumbered tertiary aliphatic amines including diethylmethylamine,[15] triethylamine,[15,16] dibenzylmethylamine,[1] tribenzylamine,[17] isopropyldimethylamine,[18] isopropylethylmethylamine,[19] 2-butylethylmethylamine,[20] and a series of *tert*-butyldialkylamines.[4] In *tert*-butylethylmethylamine and related *tert*-butyldialkylamines,

[⊗] Abstract published in *Advance ACS Abstracts*, December 1, 1995.

(1) For a recent review, see: Bushweller, C. H. In *Acyclic Organonitrogen Stereodynamics*; Lambert, J. B., Takeuchi, Y., Eds.; VCH Publishers: New York, 1992.

(2) For previous reviews, see: Lambert, J. B. *Top. Stereochem.* **1971**, *6*, 19. Lehn, J. M. *Fortschr. Chem. Forsch.* **1970**, *15*, 311. Payne, P. W.; Allen, L. C. In *Applications of Electronic Structure Theory*; Schaefer, H. F., Ed.; Plenum Press: New York, 1977; Vol. 4. Rauk, A.; Allen, L. C.; Mislow, K. *Angew. Chem., Int. Ed. Engl.* **1970**, *9*, 400.

(3) Orville-Thomas, W. J., Ed. *Internal Rotation in Molecules*; J. Wiley and Sons: New York, 1974.

(4) Bushweller, C. H.; Anderson, W. G.; Stevenson, P. E.; Burkey, D. L.; O'Neil, J. W. *J. Am. Chem. Soc.* **1974**, *96*, 3892. Also see: Bushweller, C. H.; Anderson, W. G.; Stevenson, P. E.; O'Neil, J. W. *J. Am. Chem. Soc.* **1975**, *97*, 4338.

(5) (a) Tsuboi, M.; Hirakawa, A. Y.; Tamagake, K. J. *J. Mol. Spectrosc.* **1967**, *22*, 272. (b) Nishikawa, T.; Itoh, T.; Shimoda, K. *J. Am. Chem. Soc.* **1977**, *99*, 5570. (c) Wollrab, J. W.; Laurie, V. W. *J. Chem. Phys.* **1968**, *48*, 5058. (d) Erlandson, G.; Gurdy, W. *Phys. Rev.* **1957**, *10*, 513. (e) Lide, D. R.; Mann, D. E. *J. Chem. Phys.* **1958**, *28*, 572.

(6) Durig, J. R.; Li, Y. S. *J. Chem. Phys.* **1975**, *63*, 4110. Tsuboi, M.; Tamagake, K. J.; Hirakawa, A. Y.; Yamaguchi, J.; Nakagava, H.; Manocha, A. S.; Tuazon, E. C.; Fateley, W. G. *J. Chem. Phys.* **1975**, *63*, 5177.

(7) Krueger, P. J.; Jan, J. *Can. J. Chem.* **1970**, *48*, 3229.

(8) Durig, J. R.; Compton, D. A. C. *J. Phys. Chem.* **1979**, *83*, 2873.

(9) Durig, J. R.; Cox, F. O. *J. Mol. Struct.* **1982**, *95*, 85.

(10) Swalen, J. D.; Ibers, J. A. *Chem. Phys.* **1962**, *36*, 1914.

(11) Tsuboi, M.; Hirakawa, A. Y.; Takamitsu, I.; Sasaki, T.; Tamagake, K. J. *J. Chem. Phys.* **1964**, *41*, 2721.

(12) Weston, R. E., Jr. *J. Am. Chem. Soc.* **1954**, *76*, 2645.

(13) Oki, M. In *Applications of Dynamic NMR Spectroscopy to Organic Chemistry*; VCH Publishers: New York, 1985. Sandstrom, J. In *Dynamic NMR Spectroscopy*; Academic Press: New York, 1982. Cotton, F. A. In *Dynamic Nuclear Magnetic Resonance Spectroscopy*; Academic Press: New York, 1975.

(14) Burkert, U.; Allinger, N. L. *Molecular Mechanics*; American Chemical Society: Washington, DC, 1984. Allinger, N. L. *Adv. Phys. Org. Chem.* **1976**, *13*, 1.

(15) Bushweller, C. H.; Fleischman, S. H.; Grady, G. L.; McGoff, P.; Rithner, C. D.; Whalon, M. R.; Brennan, J. G.; Marcantonio, R. P.; Domingue, R. P. *J. Am. Chem. Soc.* **1982**, *104*, 6224.

(16) Fleischmann, S. H.; Weltin, E. E.; Bushweller, C. H. *J. Comput. Chem.* **1985**, *6*, 249.

(17) Fleischman, S. H.; Whalon, M. R.; Rithner, C. D.; Grady, G. L.; Bushweller, C. H. *Tetrahedron Lett.* **1982**, 4233.

(18) Brown, J. H.; Bushweller, C. H. *J. Am. Chem. Soc.* **1992**, *114*, 8153.

(19) Brown, J. H.; Bushweller, C. H. *J. Phys. Chem.* **1994**, *98*, 11411.

(20) Danehey, C. T., Jr.; Grady, G. L.; Bonneau, P. R.; Bushweller, C. H. *J. Am. Chem. Soc.* **1988**, *110*, 7269.

0002-7863/95/1517-12567$09.00/0

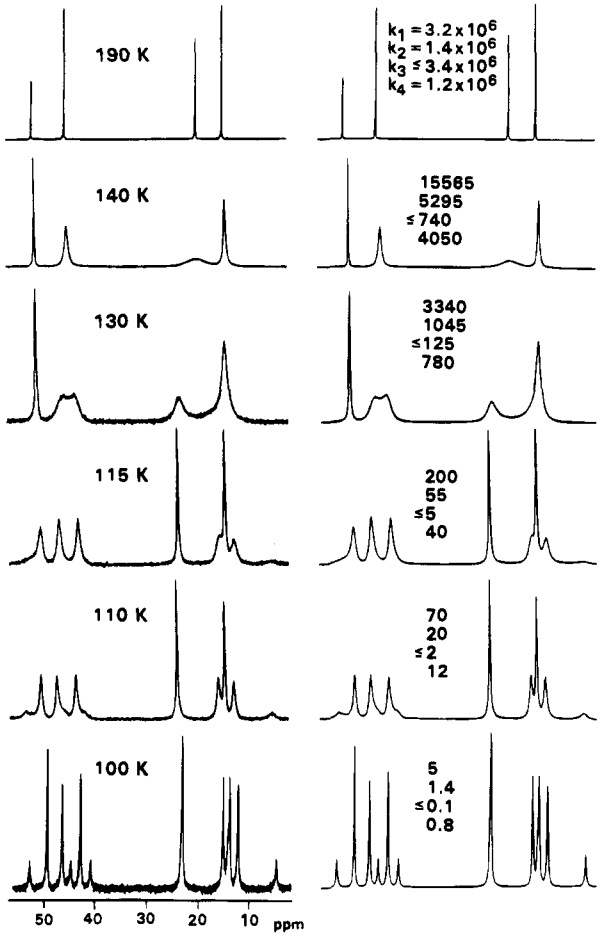

Figure 1. Experimental $^{13}C\{^1H\}$ DNMR spectra (62.898 MHz) of 2-(diethylamino)propane (**DEAP**; 3% v/v in $CBrF_3$) in the left column and theoretical simulations in the right column. The rate constants are defined in Scheme 1.

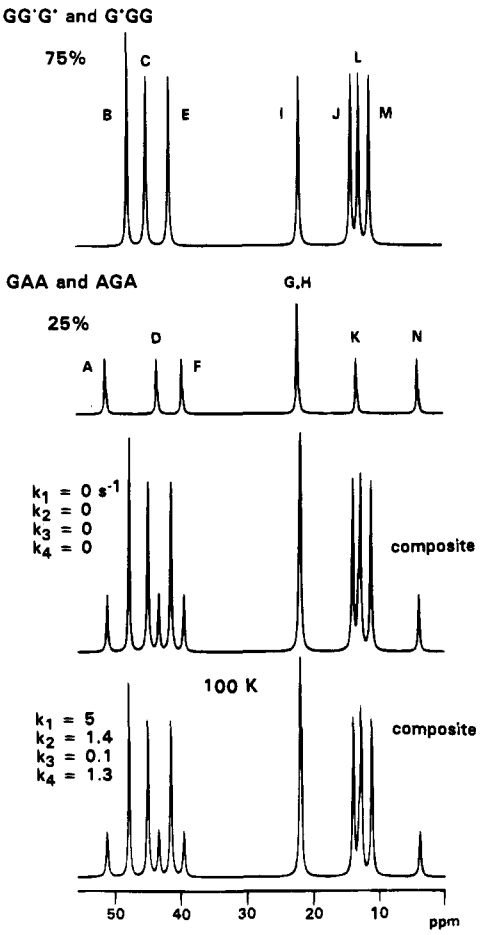

Figure 2. Decomposition of the theoretical simulation of the $^{13}C\{^1H\}$ NMR spectrum of 2-(diethylamino)propane (**DEAP**) at 100 K. The upper two subspectra are assigned to specific conformations as indicated. The upper composite spectrum is calculated with all rate constants equal to zero. The bottom composite spectrum is computed by using the rate constants necessary to obtain an accurate fit of the experimental spectrum at 100 K.

the *tert*-butyl methyl groups exchange molecular sites via a concerted *tert*-butyl rotation/nitrogen inversion process.[4] Steric crowding will decrease the pyramidality at nitrogen. Triisopropylamine prefers a conformation that has C_{3h} symmetry with an essentially trigonal planar nitrogen atom and all three methine C−H bonds in the trigonal plane.[21] In sterically crowded systems such as $(CH_3CH_2)_2CHN(i\text{-}C_3H_7)$[22] and $(t\text{-}C_4H_9)_2CHN\text{-}(CH_3)$,[23] DNMR studies revealed significant barriers to isolated rotation about carbon−nitrogen bonds on an essentially trigonal planar nitrogen template.

A number of factors will determine the relative energies of the equilibrium conformations of a tertiary aliphatic amine including the pyramidality at nitrogen and a variety of nonbonded repulsions.[1,2] In particular, *syn*-1,5 repulsions between two substituents are usually highly destabilizing.[1] When the N-substituents on a tertiary aliphatic amine become sterically larger and more branched, the possibility of *syn*-1,5 orientations between two substituents increases, more equilibrium conformations are destabilized, and fewer equilibrium conformers will be present at concentrations high enough to be NMR detectable. This paper reports DNMR studies of 2-(diethylamino)propane (**DEAP**) and 2-(dibenzylamino)propane (**DBAP**) that do reveal a limited number of equilibrium conformations that are stable enough to be NMR detectable. The NMR spectrum at 100 K shows two diastereomeric pairs of enantiomeric conformations for **DEAP** and just one pair of enantiomeric forms for **DBAP**. Molecular mechanics calculations of the relative energies of the equilibrium conformations are in good agreement with experiment.[24]

2-(Diethylamino)propane

The $^{13}C\{^1H\}$ NMR spectrum (62.9 MHz) of 2-(diethylamino)-propane (**DEAP**; 3% v/v in $CBrF_3$) at 190 K shows four singlets at δ 13.35 (methyl carbons on the ethyl groups), δ 18.44 (methyl carbons on the isopropyl group), δ 43.64 (methylene carbons), and δ 49.92 (methine carbon) as illustrated in Figure 1. Below 140 K, a complex decoalescence occurs. Slow exchange conditions are reached at 100 K. At 100 K, an accurate, complete line shape simulation requires the use of two unequally populated subspectra.[25] The two separate subspectra are illustrated at the top of Figure 2. The ^{13}C NMR chemical shifts for all resonances in each subspectrum are compiled in Table 1. Superposition of the properly weighted upper two subspectra produces the composite spectrum under conditions of no exchange of magnetization (second spectrum from bottom in Figure 2). Extrapolation of rate constants determined from

(21) Bock, H.; Coebel, I.; Havlas, Z.; Liedle, S.; Oberhammer, H. *Angew. Chem., Int. Ed. Engl.* **1991**, *30*, 187.
(22) Lunazzi, L.; Macciantelli, D.; Grossi, L. *Tetrahedron* **1983**, *39*, 305.
(23) Berger, P. A.; Hobbs, C. F. *Tetrahedron Lett.* **1978**, 1905.
(24) Allinger, N. L. *QCPE* **1987**, Program No. MM2(87). Profeta, S., Jr.; Allinger, N. L. *J. Am. Chem. Soc.* **1985**, *107*, 1907.
(25) Brown, J. H.; Bushweller, C. H. *QCPE* **1993**, Program No. 633. For a PC-based program to plot the DNMR spectra, see: Brown, J. H. *QCPE* **1993**, Program No. QCMP 123.

Table 1. ^{13}C NMR Chemical Shifts for the Stable, Equilibrium Conformations of **DEAP**[a]

	conformations[c]	
carbon(s)[b]	**GG'G'** and **G'GG** (75%)	**AGA** and **GAA** (25%)
$CH(C^*H_3)_2$	δ_I 21.86[d]	δ_G 22.02[d]
	δ_M 11.13[e]	δ_H 22.02[d]
$C^*H(CH_3)_2$	δ_B 47.85	δ_A 50.88
$CH_2C^*H_3$	δ_J 13.91[d]	δ_K 13.08[d]
	δ_L 12.72[d]	δ_N 3.81[e]
$C^*H_2CH_3$	δ_C 44.99	δ_D 43.32
	δ_E 41.49	δ_F 39.50

[a] 100 K in $CBrF_3$, spectra referenced to TMS at 0 ppm. [b] Indicated by an asterisk. [c] See Scheme 1 and Figure 2 for spectral decomposition at 100 K. [d] Gauche-to-nitrogen lone pair. [e] Anti-to-nitrogen lone pair.

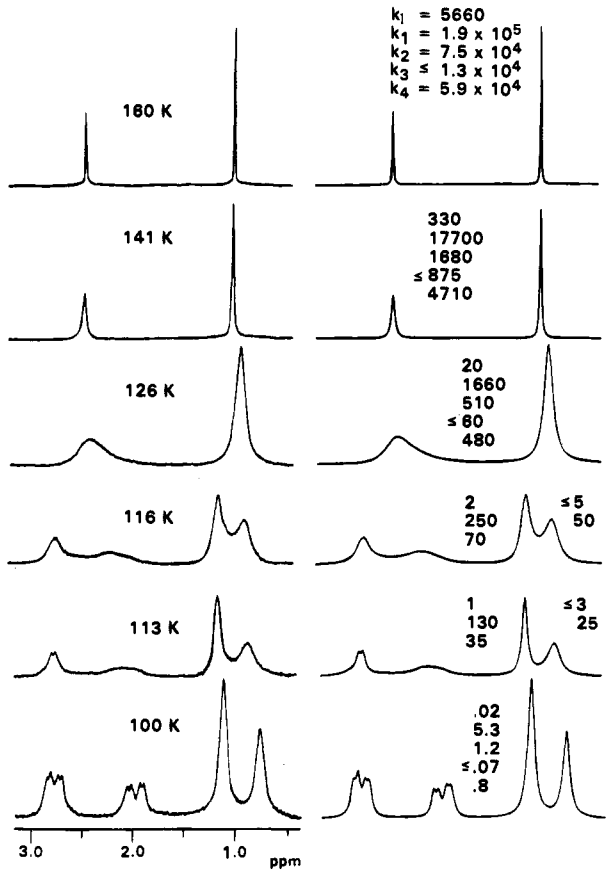

Figure 3. Experimental ^1H DNMR spectra (270 MHz) of $(CH_3)_2CDN(CH_2CD_3)_2$ (**DEAP-d_7**; 3% v/v in $CBrF_3$) in the left column and theoretical simulations in the right column. The rate constant k_i is assigned to inversion−rotation. All other rate constants are defined in Scheme 1.

simulation of the exchange broadened spectra at higher temperatures provided the rate constants used to calculate the bottom composite theoretical spectrum in Figure 2 that gives an accurate fit to the experimental spectrum at 100 K.

The ^1H DNMR spectra (270 MHz) of $(CH_3)_2CDN(CH_2CD_3)_2$ (**DEAP-d_7**; 3% v/v in $CBrF_3$) provided additional insight into the stereodynamics of **DEAP**. For **DEAP-d_7**, certain ^1H NMR signals and all vicinal proton−proton spin−spin coupling is removed resulting in useful spectral simplification. Below about 150 K, ^2H quadrupole-induced longitudinal relaxation decouples ^2H from ^1H resulting in the elimination of all vicinal spin−spin coupling at very low temperatures.[26] At 160 K, the

(26) Beall, H.; Bushweller, C. H. *Chem. Rev.* **1973**, *73*, 465. Also see: Mantsch, H. H.; Saito, H.; Smith, I. C. P. *Prog. Nucl. Magn. Reson. Spectrosc.* **1977**, *11*, 211.

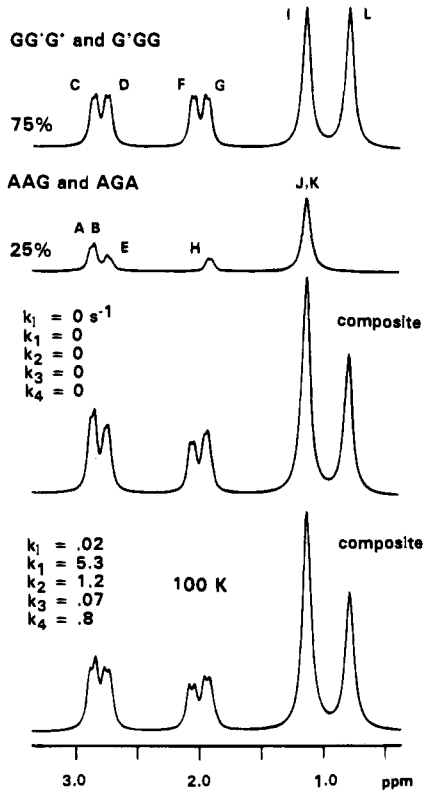

Figure 4. Decomposition of the theoretical simulation of the ^1H NMR spectrum (270 MHz) of $(CH_3)_2CDN(CH_2CD_3)_2$ (**DEAP-d_7**) at 100 K. The format for presentation of the subspectra and composite spectra is identical to that in Figure 2.

Table 2. ^1H NMR Parameters for the Stable, Equilibrium Conformations of **DEAP-d_7**[a]

	conformations[c]	
proton(s)[b]	**GG'G'** and **G'GG** (75%)	**AGA** and **GAA** (25%)
$CD(CH^*_3)_2$	δ_I 1.12[d]	δ_J 1.12[d]
	δ_L 0.78[e]	δ_K 1.12[d]
$CH^*_2CD_3$	δ_C 2.84[d]	δ_A 2.84[d]
	δ_F 2.05[e]	δ_H 1.90[e]
	($^2J_{CF} = -13.0$ Hz)	($^2J_{AH} = -13.0$ Hz)
$CH^*_2CD_3$	δ_D 2.73[d]	δ_B 2.84[d]
	δ_G 1.93[e]	δ_E 2.71[d]
	($^2J_{DG} = -13.0$ Hz)	($^2J_{BE} = -13.0$ Hz)

[a] 100 K in $CBrF_3$, spectra referenced to TMS at 0 ppm. [b] Indicated by an asterisk. [c] See Scheme 1 and Figure 4 for spectral decomposition at 100 K. [d] Gauche-to-nitrogen lone pair. [e] Anti-to-nitrogen lone pair.

spectrum of **DEAP-d_7** shows two singlets at δ 0.99 [$CD(CH_3)_2$] and δ 2.49 [$(CH_2CD_3)_2$] as shown in Figure 3. Below 130 K, the spectrum undergoes a complex decoalescence. While symmetry considerations reveal that the methylene proton resonances can serve to detect inversion at nitrogen,[1] there are no obvious separate decoalescence phenomena over distinctly different temperature ranges due to slowing inversion and to slowing isolated rotation. Barriers to inversion and to isolated rotation processes are similar in magnitude. At 100 K, an accurate complete line shape simulation requires the use of two unequally populated subspectra.[25] The two subspectra are illustrated at the top of Figure 4. The ^1H NMR chemical shifts for all resonances and coupling constants in each subspectrum are compiled in Table 2. Superposition of the properly weighted subspectra produces the composite spectrum under conditions of no exchange of magnetization (second spectrum from the bottom in Figure 4). Extrapolation from the exchange broadened temperature region provides the rate constants for the

Scheme 1. Stable Equilibrium Conformations of 2-(Diethylamino)propane (**DEAP**)

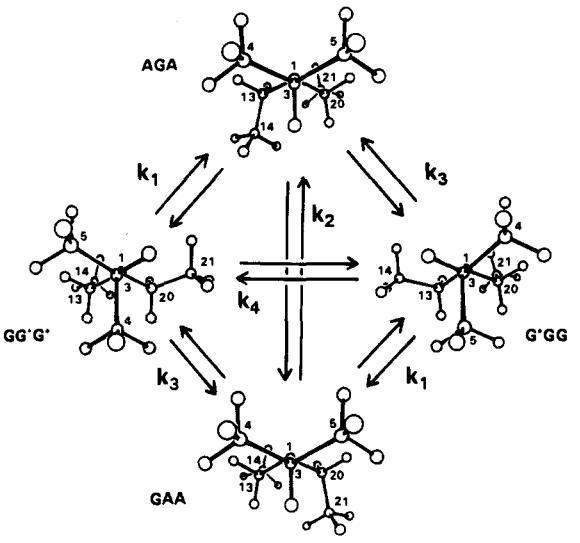

various exchange processes that are incorporated into calculation of the bottom composite theoretical spectrum in Figure 4 that gives an accurate fit of the experimental spectrum at 100 K.

The $^{13}C\{^1H\}$ NMR spectrum at 100 K can be used in conjunction with the ^1H NMR spectrum at 100 K to identify the stable, NMR-detectable equilibrium conformations of **DEAP**. A three-letter designation will be used to name the various conformations. The first two letters define the orientation of the two ethyl methyl groups (**G** denotes gauche to the lone pair and to the other ethyl group; **G′** denotes gauche to the lone pair and to the isopropyl group; **A** denotes anti to the lone pair). With the isopropyl group pointing toward the reader, the first letter refers to the ethyl group that is to the reader's left. The second letter refers to the ethyl group that is to the reader's right. The third letter defines the orientation of the isopropyl methine proton (**G** denotes gauche to the lone pair and to the ethyl group at the reader's left; **G′** denotes gauche to the lone pair and to the ethyl group at the reader's right; **A** denotes anti to the lone pair).

The major $^{13}C\{^1H\}$ NMR subspectrum (75%; Figure 2; Table 1) shows two well-separated isopropyl methyl resonances at δ_I 21.86 and δ_M 11.13. Based on established ^{13}C NMR chemical shift trends, the signal at δ_I 21.86 is assigned to a methyl group that is gauche to the lone pair and δ_M 11.13 to a methyl group that is anti to the lone pair.[18,19] The major ^1H NMR subspectrum of **DEAP-*d*$_7$** (75%; Figure 4; Table 2) also shows two well-separated isopropyl methyl signals. Based on established ^1H NMR chemical shift trends, the resonance at δ_I 1.12 is assigned to a methyl group that is gauche to the lone pair and δ_L 0.78 to a methyl group that is anti to the lone pair.[4,18,19] For the conformation(s) associated with the major subspectrum, one isopropyl methyl group must be anti to the lone pair and one gauche. *The isopropyl methine proton is in the* **G** *or* **G′** *orientation.* This precludes the **AGG**, **AGG′**, **GAG**, and **GAG′** conformations in which an ethyl methyl group adopts an **A** orientation resulting in seriously destabilizing *syn*-1,5-dimethyl repulsions between the anti ethyl methyl and anti isopropyl methyl groups. This also precludes the **G′G′G′**, **G′GG′**, **G′G′G**, and **GG′G** conformations that contain destabilizing *syn*-1,5-dimethyl repulsions between ethyl methyl and isopropyl methyl groups that are gauche to the lone pair. In fact, with one isopropyl methyl group anti and the other gauche, the only stable equilibrium conformations that avoid destabilizing *syn*-1,5-dimethyl repulsions are the enantiomeric **GG′G′** and **G′GG** forms (Scheme 1). In addition, the major $^{13}C\{^1H\}$ NMR subspectrum shows two ethyl methyl resonances at δ_J 13.91 and δ_L 12.72 (Figure 2; Table 1). Based again on established ^{13}C NMR chemical shift trends, these chemical shifts are typical of ethyl methyl groups that are oriented gauche to the nitrogen lone pair.[19] The chemical shifts of one ethyl methyl carbon (δ_J 13.91) and one methylene carbon (δ_E 41.49) are very close to the corresponding chemical shifts (δ 13.83; δ 41.10) due to the ethyl group in the **GG** conformation of 2-(ethylmethylamino)propane shown below.[19] In the **GG** form, the ethyl group

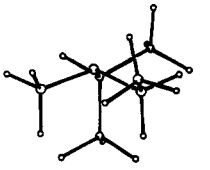

GG

is "locked" in a conformation that is strictly analogous to the **G** ethyl group of the **GG′G′** or **G′GG** conformation of **DEAP**. Therefore, the **DEAP** chemical shifts at δ_J 13.91 and δ_E 41.49 are assigned to the **G** ethyl group of the **GG′G′** and **G′GG** conformations. In the major ^1H NMR subspectrum at 100 K, the methylene protons show two well-separated CF ($\Delta\delta$ 0.79) and DG ($\Delta\delta$ 0.80) subspectra (Figure 4; Table 2). In light of the fact that the chemical shift difference between methylene protons that are oriented anti and gauche to the lone pair is about 1 ppm, the two well-separated CF and DG subspectra are strongly consistent with the **GG′G′** and **G′GG** conformations in which both ethyl methyl groups are oriented gauche to the lone pair.[1,15,19,27] One is led inexorably to assign the enantiomeric **GG′G′** and **G′GG** conformations (Scheme 1) to the major subspectrum.

The minor $^{13}C\{^1H\}$ NMR subspectrum (25%; Figure 2; Table 1) shows one resonance due to both isopropyl methyl groups at $\delta_{G,H}$ 22.02 consistent with both isopropyl methyl groups being oriented gauche to the lone pair.[18,19] The corresponding ^1H NMR subspectrum of **DEAP-*d*$_7$** at 100 K (25%; Figure 4; Table 2) also shows one isopropyl methyl signal at $\delta_{J,K}$ 1.12 consistent again with both isopropyl methyl groups being located gauche to the lone pair.[18,19] *The isopropyl methine proton must be in the* **A** *orientation.* Since both isopropyl methyl groups are gauche to the lone pair, this precludes conformations that have an ethyl methyl group in the **G′** orientation resulting in a destabilizing *syn*-1,5-dimethyl repulsion. Indeed, with both isopropyl methyl groups oriented gauche to the lone pair, the only equilibrium conformations that avoid destabilizing *syn*-1,5-dimethyl repulsions are the enantiomeric **AGA** and **GAA** forms (Scheme 1) in which the ethyl methyl groups respectively occupy **A** and **G** positions. Consistent with this rationale, a salient characteristic of the minor $^{13}C\{^1H\}$ NMR subspectrum is an ethyl methyl resonance at δ_N 3.81 (Figure 2; Table 1). This chemical shift is 8−9 ppm to lower frequency (higher field) than those for ethyl methyl groups that are gauche to the lone pair (Figure 2; Table 1) and is typical of an ethyl methyl group that is anti to the lone pair.[19] This chemical shift at δ_N 3.81 is assigned to the **A** ethyl group of the **AGA** and **GAA** conformations. The minor ^1H NMR subspectrum of the methylene protons of **DEAP-*d*$_7$** at 100 K shows both a well-separated AH subspectrum ($\Delta\delta$ 0.94) and a closely spaced BE subspectrum ($\Delta\delta$ 0.13) (Figure 4; Table 2). The well-separated AH sub-

(27) Hamlow, H. P.; Okuda, S. *Tetrahedron Lett.* **1964**, *37*, 2553. Lambert, J. B.; Keske, R. G.; Carhart, R. E.; Jovanovich, A. P. *J. Am. Chem. Soc.* **1967**, *89*, 3761.

Table 3. Relative Free Energies of the Stable, Equilibrium Conformations of **DEAP** Determined by $^{13}C\{^1H\}$ NMR Spectroscopy

conformers[a]	rel free energy (kcal/mol)[b]
GG'G' or **G'GG**	0.0
AGA or **GAA**	0.22 ± 0.02

[a] See Scheme 1. [b] At 100 K.

spectrum reveals an ethyl group that is "locked" in the **G** orientation. The methylene protons are oriented respectively anti and gauche to the lone pair.[1,15,19,27] The closely spaced BE subspectrum reveals an ethyl group that has both methylene protons gauche to the lone pair; the methyl group is in the **A** orientation. The minor subspectrum must be assigned to the **GAA** and **AGA** enantiomers (Scheme 1).

For **DEAP**, the ^1H and $^{13}C\{^1H\}$ DNMR spectra both reveal a small *free energy* preference (0.22 kcal/mol at 100 K) for the **GG'G'** or **G'GG** conformation over the **AGA** or **GAA** form (Table 3).

Theoretical simulations of the $^{13}C\{^1H\}$ and ^1H DNMR spectra allowed identification of the preferred pathways for conformational exchange in **DEAP**.[25] In the regions of intermediate rates of exchange, the DNMR line shape will be determined by those rates of magnetization transfer that are associated with the minimum energy or preferred pathways (faster rates) for conformational interconversion. Therefore, the approach used in simulating the DNMR spectra was to start at 100 K where all rates are very slow and, as the sample temperature increased, to turn on only those rates that are necessary and sufficient to achieve an accurate complete line shape simulation.

For the $^{13}C\{^1H\}$ DNMR spectra, the most rapid process involves exchange between BMI and AGH (or AHG) sets of resonances for the isopropyl group, while the two ethyl groups show exchange between CL and DK as well as EJ and FN sets of chemical shifts. The BMI to AGH (or AHG), CL to DK, and EJ to FN transfers are associated with the **GG'G'** to **AGA** (or **G'GG** to **GAA**) conformational interconversion (k_1; Scheme 1). The BMI to AGH (or AHG) transfer corresponds to a **G'** (or **G**) to **A** conversion for the isopropyl group; the EJ to FN transfer corresponds to a **G** to **A** conversion for one ethyl methyl group; the CL to DK transfer corresponds to a **G'** to **G** conversion for the other ethyl methyl group. The free energy of activation for this process is 5.3 ± 0.1 kcal/mol at 115 K. Listed in Table 4 are all the magnetization transfers and assigned conformational exchanges invoked to simulate the spectra. All measured free energies of activation are also listed in Table 4.

Racemization of the **GAA** and **AGA** enantiomers (k_2 and the reverse reaction; Scheme 1) involves exchanges of magnetization between DK and FN, as well as FN and DK, sets of resonances for the two ethyl groups (Tables 1 and 4). Since the chemical shifts of the resonances due to the isopropyl methyl groups in the **GAA** and **AGA** conformations are identical (Table 1), they are not affected by this exchange process and cannot be used as a probe of the exchange. The free energy of activation for this process is 5.6 ± 0.2 kcal/mol at 115 K.

Racemization of the **GG'G'** and **G'GG** enantiomers (k_4 and the reverse reaction; Scheme 1) involves exchange between BIM and BMI sets of resonances for the isopropyl group, while the ethyl groups show exchanges of magnetization between EJ and CL, as well as CL and EJ, sets of chemical shifts (Table 4). The free energy of activation for this process is 5.7 ± 0.2 kcal/mol at 115 K.

Although it is reasonable to presume that conformational exchange between the **GG'G'** and **GAA** (or **G'GG** and **AGA**) conformations occurs (k_3 and the reverse reaction; Scheme 1),

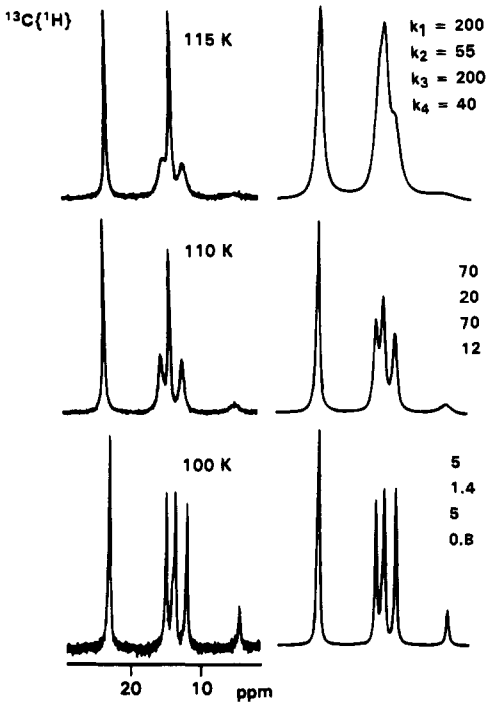

Figure 5. Experimental $^{13}C\{^1H\}$ DNMR spectra (62.898 MHz) of 2-(diethylamino)propane (**DEAP**; 3% v/v in $CBrF_3$) in the left column and theoretical simulations with $k_1 = k_3$ in the right column. The rate constants are defined in Scheme 1.

accurate fits of the DNMR spectra did not require invoking these processes in the line shape calculations. It is apparent that these processes occur at a rate that is sufficiently slower than other processes that they do not affect the DNMR line shape. In order to assign a lower limit to $\Delta G^{\ddagger}$ for the k_3 process, theoretical $^{13}C\{^1H\}$ DNMR spectra at specific temperatures were calculated by leaving k_1, k_2, and k_4 at values that gave accurate spectral fits and progressively increasing k_3 until there was a clearly discernible discrepancy between the theoretical and experimental spectra. The upper limits for k_3 that still produce acceptable fits at 130, 115, and 110 K are shown on Figure 1. Any rate above this upper limit gives unacceptable results. The upper limits for k_3 at 190, 140, and 100 K were obtained by a least-squares extrapolation of upper limits at other temperatures. Any attempt to use equal values for k_1 and k_3 gave clearly unacceptable results (Figure 5). At 115 K, the upper limit for k_3 is 5 s^{-1}, giving a lower limit on $\Delta G^{\ddagger}$ of 6.2 ± 0.3 kcal/mol.

The ^1H DNMR spectra of **DEAP-d_7** (Figure 3) were simulated by using virtually the same kinetic model as that used for the $^{13}C\{^1H\}$ DNMR spectra except that, above 116 K, it became necessary to turn on random exchange of all resonances due to each methylene group in all conformations. For symmetry reasons, the methylene protons in one invertomer of **DEAP** are diastereotopic. Their molecular environments can be mutually interchanged only by inversion−rotation at the pyramidal nitrogen.[1] The necessity to invoke random exchange of the methylene protons signals reflects the onset of inversion−rotation at nitrogen and is associated with rate constant k_i ($\Delta G^{\ddagger}$ = 6.4 ± 0.2 kcal/mol at 123 K) in Figure 3. All other rate constants are defined in Scheme 1. Magnetization transfers, assigned conformational conversions, and $\Delta G^{\ddagger}$ values are listed in Table 5. Although the reduced chemical shift dispersion associated with the ^1H DNMR spectra led to more subspectral overlap and caused some problems with the line shape simulations, the agreement with the data derived from the $^{13}C\{^1H\}$ DNMR spectra is excellent (Tables 4 and 5).

Table 4. Barriers to Isolated Rotation about Carbon−Nitrogen Bonds in **DEAP** Measured by $^{13}C\{^1H\}$ DNMR Spectroscopy

substituent	magnetization transfer[a]	rate constant,[b] s^{-1}	conform exchange[b]	$\Delta G^{\ddagger}$(temp),[c] kcal/mol
$CH(CH_3)_2$	BMI to AGH (or AHG)	k_1	**GG'G'** to **AGA** (or **G'GG** to **GAA**)	5.3 ± 0.1
CH_2CH_3	EJ to FN	k_1	**GG'G'** to **AGA** (or **G'GG** to **GAA**)	5.3 ± 0.1
CH_2CH_3	CL to DK	k_1	**GG'G'** to **AGA** (or **G'GG** to **GAA**)	5.3 ± 0.1
CH_2CH_3	DK to FN	k_2	**GAA** to **AGA**	5.6 ± 0.2
CH_2CH_3	FN to DK	k_2	**GAA** to **AGA**	5.6 ± 0.2
$CH(CH_3)_2$	BMI to AGH (or AHG)	k_3	**GG'G'** to **GAA** (or **G'GG** to **AGA**)	≥6.2 ± 0.3
CH_2CH_3	EJ to DK	k_3	**GG'G'** to **GAA** (or **G'GG** to **AGA**)	≥6.2 ± 0.3
CH_2CH_3	CL to FN	k_3	**GG'G'** to **GAA** (or **G'GG** to **AGA**)	≥6.2 ± 0.3
$CH(CH_3)_2$	BIM to BMI	k_4	**GG'G'** to **G'GG**	5.7 ± 0.2
CH_2CH_3	EJ to CL	k_4	**GG'G'** to **G'GG**	5.7 ± 0.2
CH_2CH_3	CL to EJ	k_4	**GG'G'** to **G'GG**	5.7 ± 0.2

[a] See Table 1 and Figures 1 and 2. [b] See Scheme 1. [c] Calculated at 115 K. For all processes, $\Delta S^{\ddagger} = 0 \pm 3$ cal/(mol·K).

Table 5. Barriers to Isolated Rotation about Carbon−Nitrogen Bonds in **DEAP** Measured by ^1H DNMR Spectroscopy

substituent	magnetization transfer[a]	rate constant,[b] s^{-1}	conform exchange[b]	$\Delta G^{\ddagger}$(temp), kcal/mol[c]
$CD(CH_3)_2$	IL to JK (or KJ)	k_1	**GG'G'** to **AGA** (or **G'GG** to **GAA**)	5.3 ± 0.1
CH_2CD_3	DG to EB	k_1	**GG'G'** to **AGA** (or **G'GG** to **GAA**)	5.3 ± 0.1
CH_2CD_3	CF to HA	k_1	**GG'G'** to **AGA** (or **G'GG** to **GAA**)	5.3 ± 0.1
CH_2CD_3	AH to EB	k_2	**GAA** to **AGA**	5.6 ± 0.2
CH_2CD_3	BE to HA	k_2	**GAA** to **AGA**	5.6 ± 0.2
$CD(CH_3)_2$	IL to KJ (or JK)	k_3	**GG'G'** to **GAA** (or **G'GG** to **AGA**)	≥6.2 ± 0.3
CH_2CD_3	DJ to AG	k_3	**GG'G'** to **GAA** (or **G'GG** to **AGA**)	≥6.2 ± 0.3
CH_2CD_3	CF to BE	k_3	**GG'G'** to **GAA** (or **G'GG** to **AGA**)	≥6.2 ± 0.3
$CD(CH_3)_2$	IL to LI	k_4	**GG'G'** to **G'GG**	5.6 ± 0.2
CH_2CD_3	DG to FC	k_4	**GG'G'** to **G'GG**	5.6 ± 0.2
CH_2CD_3	CF to GD	k_4	**GG'G'** to **G'GG**	5.6 ± 0.2

[a] Table 1 and Figure 4. [b] Scheme 1. [c] Calculated at 116 K.

As simulations of the ^1H DNMR spectra of **DEAP-d_7** show (*vide supra*), the free energy of activation for nitrogen inversion in **DEAP** is 6.4 ± 0.2 kcal/mol at 123 K. Therefore, those conformational exchanges that have rates faster than inversion (k_1, k_2, and k_4 in Scheme 1) do indeed occur by multiple isolated rotations about carbon−nitrogen bonds as shown in Scheme 1. Because the barrier could not be measured accurately, the situation with regard to the conformational exchange associated with k_3 is not clear. It is possible that the barrier to interconversion between the **GG'G'** (or **G'GG**) and **GAA** (or **AGA**) forms via multiple isolated rotations is higher than that for inversion. In that instance, the **GG'G'** (or **G'GG**) conformation may be converted to the **GAA** (or **AGA**) conformation of the *other invertomer* of **DEAP** via a concerted inversion−rotation process.[1,4]

Thus, the *preferred* pathways for conformational exchange among the NMR-detectable conformations of **DEAP** via multiple isolated rotations (rate constants k_1, k_2, and k_4 and the respective back reactions) are illustrated in Scheme 1. All these conformational exchanges require at least two C−CH_3/*N*-alkyl or *N*-alkyl/*N*-alkyl eclipsings that lead to barriers high enough to be DNMR visible ($\Delta G^{\ddagger}$ = 5.3−5.7 kcal/mol). The barrier to inversion−rotation ($\Delta G^{\ddagger}$ = 6.4 ± 0.2 kcal/mol) is comparable to the lower barrier limit for one conformational exchange (k_3; Scheme 1) and only slightly higher (0.7−1.1 kcal/mol) than those for the detected isolated rotations (k_1, k_2, k_4; Scheme 1).

Molecular mechanics calculations done by using the Allinger−Profeta amine force field in the MM2(87) computer program agree well with the NMR results.[24] For each equilibrium conformation, the geometry was fully optimized using the standard Newton−Raphson energy minimization scheme. Molecular mechanics calculations predict the **GG'G'** and **G'GG** enantiomers to be the two most stable conformations each with a calculated heat of formation (ΔH_f) equal to −28.12 kcal/mol. The **AGA** and **GAA** enantiomers (ΔH_f = −27.70 kcal/mol) are predicted to be the next most stable species. Selected bond lengths, bond angles, and dihedral angles for these stable forms are compiled in Table 6. Molecular mechanics indicates a small *enthalpy* preference (0.42 kcal/mol) for the **GG'G'** and **G'GG** enantiomers over the **AGA** and **GAA** forms in very good agreement with the *free energy* preference determined by NMR at 100 K (0.22 kcal/mol). The discrepancy between the free energy difference determined by NMR and the enthalpy difference calculated by MM2 *might* reflect a small entropy preference for the **AGA** and **GAA** forms.

Those equilibrium geometries that have destabilizing *syn*-1,5-dimethyl repulsions, such as **GGA_1** (Chart 1), are MM2(87) computed to be 2.78 to 3.72 kcal/mol higher in energy than the **GG'G'** and **G'GG** forms and will not be present in concentrations high enough to be detected by NMR. In the **GGA_1** form, small torsions occur about all three carbon−nitrogen bonds in order to optimize *syn*-1,5-dimethyl repulsions. The **GGA_1** conformation interconverts with its enantiomer (**GGA_2**) via a low barrier process involving small torsions about all three nitrogen−carbon bonds (libration) and close passage of the ethyl methyl groups.[19] In Chart 1, a conformation in the left column is the enantiomer of the conformation to its immediate right. The **GGG'_1** and **GGG'_2**, and also **GGG_1** and **GGG_2**, interconvert via libration. Relative MM2(87) energies of a number of equilibrium conformers of **DEAP** are listed in Table 7.

It is interesting to note that conversion of the **GG'G'** conformation to the **AGA** form (k_1, Scheme 1) and the **GG'G'** to **GAA** conversion (k_3, Scheme 1) are topologically different processes. They involve conversion of one member of an enantiomeric pair of conformations to either member of a different pair of enantiomeric conformations. In principle, these processes could have different barriers. In fact, accurate

Table 6. Selected Dihedral Angles, Bond Angles, and Bond Lengths for the **GG'G'**, **G'GG**, **AGA**, and **GAA** Conformations (Scheme 1) of **DEAP** Calculated by Using Allinger's MM2(87) Molecular Mechanics Force Field

dihedral angle (deg)		bond angle (deg)		bond length (Å)	
		GG'G' Conformer[a]			
3−1−13−14	173.2	3−1−13	112.7	1−13	1.4640
3−1−20−21	−52.2	3−1−20	113.2	1−3	1.4691
5−3−1−20	172.3	13−1−20	110.9	1−20	1.4636
5−3−1−13	−60.7				
4−3−1−20	−61.0				
4−3−1−13	65.9				
		G'GG Conformer[a]			
3−1−13−14	52.2	3−1−13	113.2	1−13	1.4636
3−1−20−21	−173.3	3−1−20	112.8	1−3	1.4691
5−3−1−20	−66.0	13−1−20	110.9	1−20	1.4640
5−3−1−13	60.9				
4−3−1−20	60.6				
4−3−1−13	−172.4				
		AGA Conformer[a]			
3−1−13−14	−62.8	3−1−13	113.1	1−13	1.4632
3−1−20−21	179.1	3−1−20	111.6	1−3	1.4728
5−3−1−20	58.0	13−1−20	112.1	1−20	1.4646
5−3−1−13	−174.5				
4−3−1−20	179.3				
4−3−1−13	−53.2				
		GAA Conformer[a]			
3−1−13−14	−179.1	3−1−13	111.6	1−13	1.4646
3−1−20−21	62.8	3−1−20	113.1	1−3	1.4728
5−3−1−20	53.1	13−1−20	112.1	1−20	1.4632
5−3−1−13	−179.4				
4−3−1−20	174.4				
4−3−1−13	−58.1				

[a] The atomic numbering scheme is given on the **GG'G'**, **G'GG**, **AGA**, and **GAA** conformations shown in Scheme 1.

simulations of the DNMR spectra (*vide supra*) did not require invoking exchanges of magnetization between the **GG'G'** and **GAA** conformations or between the **G'GG** and **AGA** forms suggesting strongly that the barrier for the **GG'G'** to **GAA** (or **G'GG** to **AGA**) is higher than that for **GG'G'** to **AGA** (or **G'GG** to **GAA**). Attempts to determine the origin of this barrier differential by doing extensive barrier calculations using the general dihedral angle driver option in MM2(87) were not successful.

2-(Dibenzylamino)propane

The $^{13}C\{^1H\}$ NMR spectrum (62.9 MHz) of 2-(dibenzylamino)propane (**DBAP**; 2% v/v in $CBrF_3$) at 180 K shows seven singlets at δ 17.80 (isopropyl methyl carbons), δ 48.81 (isopropyl methine carbon), δ 54.05 (benzyl methylene carbons), δ 127.83 (*p*-phenyl carbons), δ 129.34 and δ 130.53 (*o*- and *m*-phenyl carbons), and δ 142.21 (quaternary phenyl carbons) as shown in Figures 6 and 7. Below 130 K, the isopropyl methyl and benzyl methylene carbon resonances each decoalesce into two signals of equal intensity while the isopropyl methine carbon resonance remains a sharp singlet down to 100 K (Figure 6). Slow-exchange conditions are reached at about 100 K. For the conformational exchange detected in Figure 6, the isopropyl methine carbon is exchanging between or among equivalent molecular environments. The isopropyl methyl carbons and the benzyl methylene carbons each undergo a mutual exchange of molecular environments. The para and quaternary phenyl carbon resonances also decoalesce into two signals of equal intensity (Figure 7). The spectrum at 100 K reveals the presence of a pair of enantiomeric conformations or at least two equivalent conformations. All ^{13}C NMR chemical shifts measured from the 100 K spectrum are listed in Table 8.

Chart 1. Selected High-Energy Equilibrium Conformations for **DEAP**

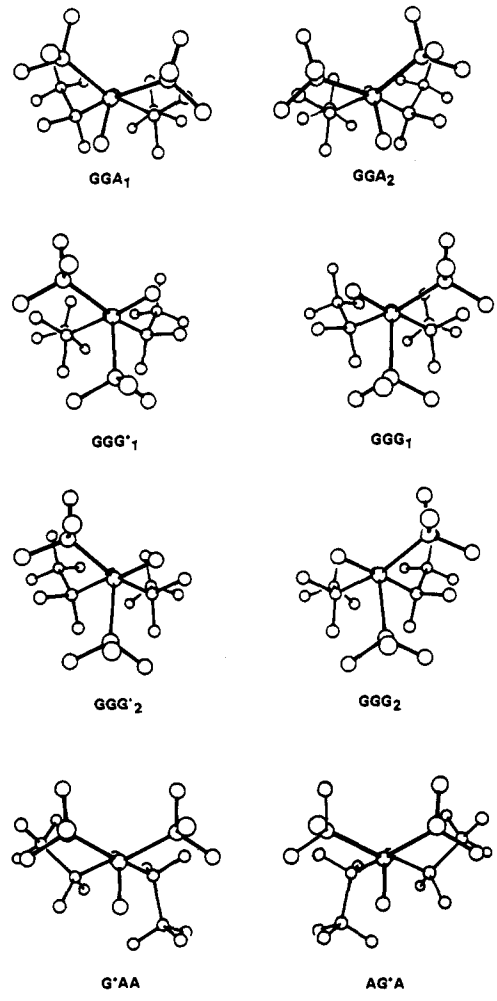

Table 7. Relative Energies of Selected Conformations of **DEAP** Calculated by Allinger's MM2(87) Molecular Mechanics Force Field

conformers	rel energy	conformers	rel energy
GG'G' or **G'GG**	0.00	**GGG$_2$** or **GGG'$_2$**	2.98
AGA or **GAA**	0.42	**G'AA** or **AG'A**	3.36
GAG' or **AGG**	2.78	**GGA$_1$** or **GGA$_2$**	3.72
GAG or **AGG'**	2.85	**G'GG'** or **GG'G**	2.85
GGG$_1$ or **GGG'$_1$**	2.86		
G'G'G' or **G'G'G**	2.96		

^1H DNMR spectra (250 MHz) of **DBAP** (2% v/v in $CBrF_3$) were also recorded. At 180 K, the ^1H NMR spectrum of **DBAP** shows a doublet (δ 1.08; $^3J_{HCCH}$ = 7.0 Hz; $(C(CH_3)_2$; 6H), a septet (δ 2.90; $^3J_{HCCH}$ = 7.0 Hz; CH; 1H), a singlet (δ 3.54; CH_2; 4H), a multiplet (δ 7.18; *p*-phenyl protons; 2H), a multiplet (δ 7.28; *m*-phenyl protons; 4H), and a multiplet (δ 7.60; *o*-phenyl protons; 4H). At 130 K, the signal due to the methylene protons is decoalesced into two differentially broadened resonances while the other resonances remain relatively sharp (Figure 8). This is consistent with slowing nitrogen inversion on the NMR chemical exchange time scale while isolated rotation about carbon−nitrogen and carbon−carbon bonds remains faster at 130 K.[1] The asymmetric shape of the resonances due to the methylene protons at 130 K is due to the onset of slowing isolated rotation about carbon−nitrogen bonds. Below 130 K, a complex decoalescence occurs due to slowing isolated rotation about carbon−nitrogen bonds (Figure 8). Slow exchange conditions are reached at 95 K. Except for broadening

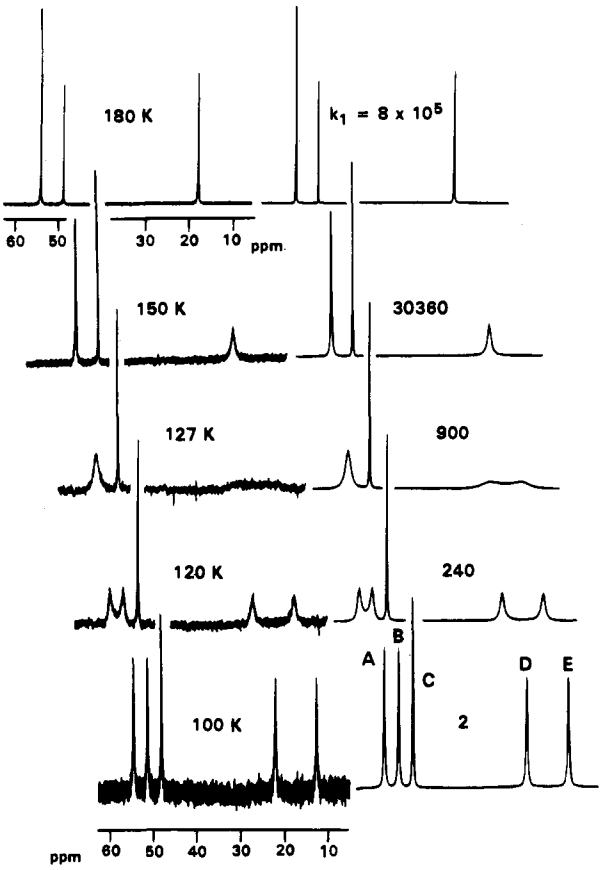

Figure 6. Experimental $^{13}C\{^1H\}$ DNMR spectra (62.898 MHz) of the aliphatic region of 2-(dibenzylamino)propane (**DBAP**; 2% v/v in $CBrF_3$) in the left column and theoretical simulations in the right column. The rate constant k_1 is defined in Scheme 2.

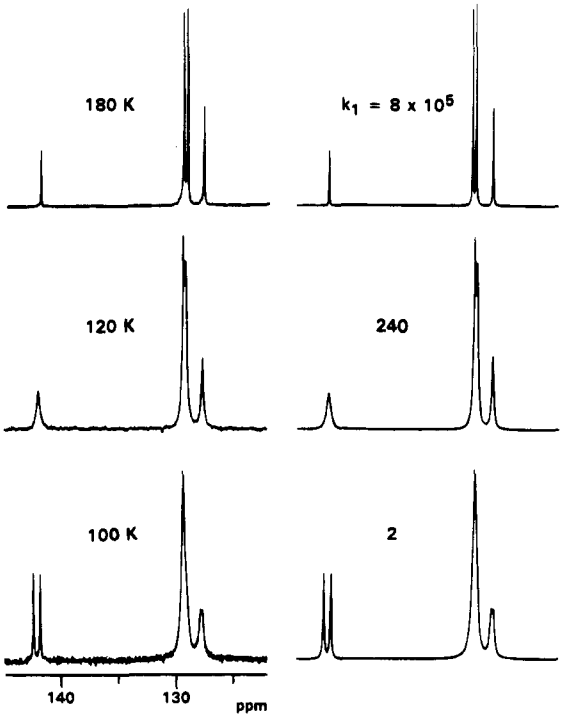

Figure 7. Experimental $^{13}C\{^1H\}$ DNMR spectra (62.898 MHz) of the phenyl region of 2-(dibenzylamino)propane (**DBAP**) in the left column and theoretical simulations in the right column. The rate constant k_1 is defined in Scheme 2.

due to more efficient transverse relaxation at low temperatures, the methine proton septet remains unchanged down to 95 K.

Table 8. ^{13}C NMR Chemical Shifts for the **G'GG** and **GG'G'** Conformations of **DBAP**[a]

carbon(s)[b]	chemical shifts (ppm)[c]
$CH(C^*H_3)_2$	δ_D 22.26[d]
	δ_E 12.72[e]
$C^*H(CH_3)_2$	δ_C 48.49
C^*H_2Ph	δ_A 55.01
	δ_B 51.75
C_6H_5	
quaternary	δ 142.69[d]
	δ 142.05[d]
para	δ 127.97
	δ 129.75
ortho or meta	δ 129.49
	δ 129.49
ortho or meta	δ 129.24
	δ 129.48

[a] 100 K in $CBrF_3$, spectra referenced to TMS at 0 ppm. [b] Indicated by an asterisk. [c] See Figure 6 for chemical shift labels. [d] Gauche-to-nitrogen lone pair. [e] Anti-to-nitrogen lone pair.

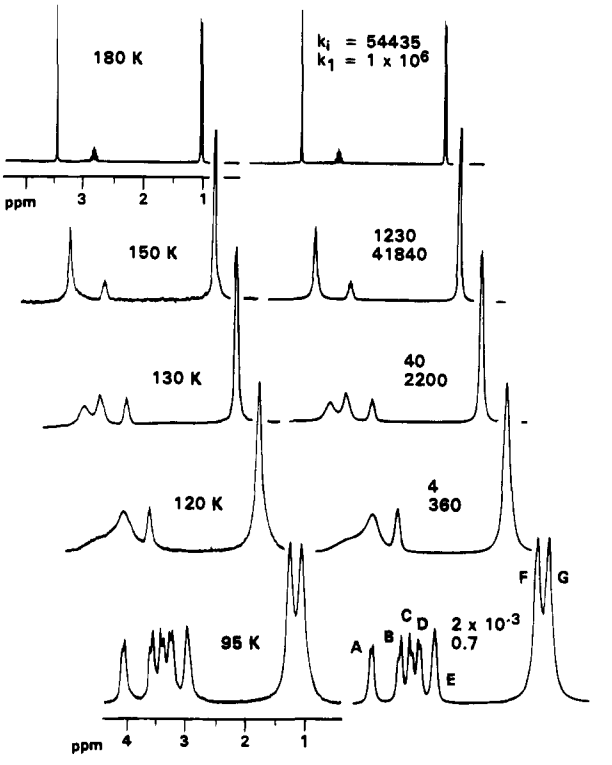

Figure 8. Experimental ^1H DNMR spectra (250 MHz) of the alkyl region of 2-(dibenzylamino)propane (**DBAP**; 2% v/v in $CBrF_3$) in the left column and theoretical simulations in the right column. The rate constant k_1 is defined in Scheme 2; k_i is the rate constant for inversion–rotation.

The ^1H NMR chemical shifts for all aliphatic protons determined from a complete line shape analysis are compiled in Table 9.[25] The ^1H NMR spectrum at 95 K shows the presence of two enantiomeric conformations or at least two equivalent conformations and is rigorously consistent with the $^{13}C\{^1H\}$ NMR spectrum at 100 K.

The $^{13}C\{^1H\}$ NMR spectrum at 100 K can be used in conjunction with the ^1H NMR spectrum at 95 K to identify the dominant conformations of **DBAP**. After replacing the ethyl methyl groups of **DEAP** with phenyl moieties, a three-letter designation that is strictly analogous to that used to name the conformations of **DEAP** (*vide supra*) will be used to name the various conformations of **DBAP**.

The $^{13}C\{^1H\}$ NMR spectrum at 100 K (Figure 6) shows two well-separated isopropyl methyl resonances at δ_D 22.26 and δ_E

Table 9. Aliphatic ^{1}H NMR Chemical Shifts for the Stable, Equilibrium Conformations of **DBAP**[a]

protons(s)[b]	chemical shifts (ppm)[c]	
$CH(CH^*_3)_2$	δ_F 1.28[d]	δ_G 1.08[e]
$CH^*(CH_3)_2$	δ_E 3.00	
	($^3J_{EF} = {}^3J_{EG} = 7.0$ Hz)	
CH^*_2Ph	δ_A 4.08	δ_B 3.60
	δ_D 3.28	δ_C 3.42
	($^2J_{AD} = {}^2J_{BC} = -12.0$ Hz)	

[a] 95 K in $CBrF_3$, spectra referenced to TMS at 0 ppm. See Scheme 2. [b] Indicated by an asterisk. [c] See Figure 8 for chemical shift labels. [d] Gauche-to-nitrogen lone pair. [e] Anti-to-nitrogen lone pair.

Scheme 2. Stable Equilibrium Conformations of 2-(Dibenzylamino)propane (**DBAP**)

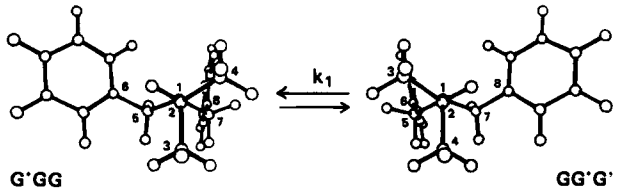

12.72 showing methyl groups that are oriented respectively gauche and anti to the lone pair.[18,19] The ^{1}H NMR spectrum at 95 K (Figure 8) also shows two isopropyl methyl signals at δ_F 1.28 and δ_G 1.08 also showing isopropyl methyl groups that are oriented respectively gauche and anti to the lone pair.[18,19] One isopropyl methyl group must be anti and the other gauche to the lone pair. *The isopropyl methine proton must be in the* **G** *or* **G'** *orientation.* The spectra at about 100 K must be assigned to the strongly dominant **G'GG** and **GG'G'** enantiomers (Scheme 2). No other diastereomeric conformations are detected in the spectrum. In the **G'GG** and **GG'G'** conformations, both phenyl groups are oriented gauche to the lone pair. The $^{13}C\{^1H\}$ NMR spectrum at 100 K (Figure 7) does indeed show two closely spaced phenyl quaternary carbon resonances at δ 142.69 and δ 142.05 indicating similar chemical environments for these carbon atoms. This is consistent with both quaternary carbons being gauche to the lone pair and inconsistent with phenyl groups being alternately anti and gauche to the lone pair in the **AGA** and **GAA** forms.

The ^{1}H NMR resonances due to the methylene protons at 95 K show well-separated AD ($\Delta\delta$ 0.80) and closely spaced BC ($\Delta\delta$ 0.32) subspectra. The widely spaced AD subspectrum is consistent with a phenyl group that is "locked" in a **G** or **G'** position with one benzyl methylene proton oriented anti (δ_D 3.28) and the other gauche (δ_A 4.08) to the lone pair.[4,15,27] Considering the fact that the NMR spectra at about 100 K reveal the essentially exclusive presence of the **G'GG** and **GG'G'** conformations, the closely spaced BC ($\Delta\delta$ 0.32) subspectrum is ostensibly inconsistent with the benzyl methylene protons being oriented anti and gauche to the lone pair. However, examination of the MM2(87)-optimized **GG'G'** and **G'GG** conformations[24] (Scheme 2) shows that the methylene proton on the **G'** benzyl group that is gauche to the lone pair may lie within the shielding region of the phenyl ring on the **G** benzyl group.[28] Differential shielding of this proton would lead to a reduction of the chemical shift difference between the methylene protons, as observed (Figure 8).

For reasons of molecular symmetry, inversion at nitrogen in **DBAP** is invisible to the $^{13}C\{^1H\}$ DNMR method.[1] In simulating the $^{13}C\{^1H\}$ DNMR spectra (Figures 6 and 7), the DNMR exchange model reflects the enantiomerization in Scheme 2. This process occurs via a series of isolated rotations about all three carbon–nitrogen bonds. For the isopropyl group, the DNMR model invoked an exchange of magnetization between CDE and CED sets of resonances (Figure 6). For each of the benzyl methylene carbons, the DNMR model used a two-site exchange between A and B chemical shifts. The free energy of activation for the enantiomerization in Scheme 2 ($\Delta G^\ddagger$ = 5.5 ± 0.1 kcal/mol at 120 K; $\Delta S^\ddagger = 0 \pm 3$ cal/(mol·K)) is very close to that for the analogous process in **DEAP** ($\Delta G^\ddagger = 5.7 \pm$ 0.2 kcal/mol at 115 K).

The ^{1}H DNMR spectra of **DBAP** (Figure 8) were simulated by using virtually the same kinetic model as that used for the $^{13}C\{^1H\}$ DNMR spectra, except that nitrogen inversion is now visible to the ^{1}H DNMR method.[1] From 95 to about 120 K, the spectra were simulated accurately by using an exchange of magnetization between EFG and EGF sets of resonances for the isopropyl group and between AD and CB sets of signals for each of the methylene groups. These exchanges correspond to the enantiomerization illustrated in Scheme 2 that occurs via isolated rotations about carbon–nitrogen bonds. The free energy of activation is 5.4 ± 0.1 kcal/mol at 120 K in good agreement with the $^{1}13C\{^1H\}$ DNMR result. For reasons of molecular symmetry, the ^{1}H NMR resonance due to the prochiral methylene protons of **DBAP** can be used as a probe of nitrogen inversion.[1] Above 120 K, accurate simulations required turning on random exchange of all signals due to the methylene protons. This random exchange reflects the onset of inversion at nitrogen and is associated with the rate constant k_i ($\Delta G^\ddagger$ = 6.4 ± 0.2 kcal/mol at 130 K) in Figure 8.[1] The barrier to inversion for **DBAP** is equal to the inversion barrier in **DEAP** ($\Delta G^\ddagger$ = 6.4 ± 0.2 kcal/mol at 123 K).

Molecular mechanics calculations do indeed indicate the **GG'G'** and **G'GG** enantiomers (Scheme 2) to be the two most stable species each with a heat of formation (ΔH_f) equal to 227.94 kcal/mol. The **AGA** and **GAA** enantiomers are predicted to be the next most stable species (ΔH_f = 230.19 kcal/mol). Selected bond lengths, bond angles, and dihedral angles for these equilibrium conformations are compiled in Table 10.

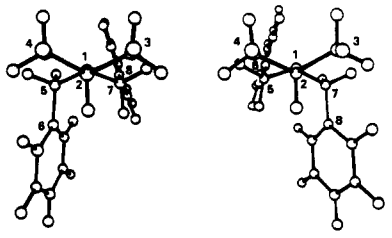

The molecular mechanics calculations predict that the **G'GG** and **GG'G'** conformations will be present essentially exclusively at 100 K (99.999%), consistent with experimental results.

Discussion

While symmetry considerations are similar for **DEAP** and **DBAP**, conformational preferences differ. For **DEAP**, there are significant concentrations of **GG'G'/G'GG** (75%) and **AGA/GAA** (25%) pairs of enantiomers at 100 K (Scheme 1). In **DBAP**, the only conformations detected by NMR at 100 K are the **GG'G'** and **G'GG** enantiomers (Scheme 2). In **DEAP**, there is a significant presence of conformations that have an ethyl methyl group anti to the lone pair (**AGA** and **GAA**). In **DBAP**, conformations that have a phenyl group anti to the lone pair are undetectable by NMR. Molecular mechanics suggests that the central CNC bond angles in **DEAP** and **DBAP** are similar

(28) Bovey, F. A. In *Nuclear Magnetic Resonance Spectroscopy*, 2nd ed.; Academic Press: New York, 1988.

Table 10. Selected Structural Parameters for the **G'GG**, **GG'G'**, **AGA**, and **GAA** Conformations of **DBAP** Calculated Using Allinger's MM2(87) Molecular Mechanics Force Field

dihedral angle (deg)		bond angle (deg)		bond length (Å)	
		G'GG Conformer[a]			
7−1−2−4	65.2	7−1−2	113.3	1−7	1.462
7−1−2−3	−61.1	7−1−5	110.2	1−2	1.468
2−1−7−8	−168.0	2−1−5	112.8	1−5	1.438
2−1−5−6	57.9				
5−1−2−4	−168.5				
5−1−2−3	65.1				
		GG'G' Conformer[a]			
7−1−2−4	−66.3	7−1−2	112.8	1−7	1.463
7−1−2−3	167.4	7−1−5	110.1	1−2	1.467
2−1−7−8	−59.2	2−1−5	113.5	1−5	1.461
2−1−5−6	164.5				
5−1−2−4	59.8				
5−1−2−3	−66.5				
		AGA Conformer[a]			
7−1−2−4	173.9	7−1−2	112.4	1−7	1.464
7−1−2−3	53.5	7−1−5	111.6	1−2	1.471
2−1−7−8	−172.8	2−1−5	114.0	1−5	1.469
2−1−5−6	−71.9				
5−1−2−4	−57.9				
5−1−2−3	−178.3				
		GAA Conformer[a]			
7−1−2−4	−175.7	7−1−2	113.5	1−7	1.469
7−1−2−3	64.4	7−1−5	111.1	1−2	1.469
2−1−7−8	59.8	2−1−5	113.9	1−5	1.438
2−1−5−6	166.1				
5−1−2−4	−47.2				
5−1−2−3	−167.1				

[a] The atomic numbering scheme is given on the **G'GG** and **GG'G'** conformations shown in Scheme 2 and on structures **AGA** and **GAA** in the text.

(Tables 6 and 10), i.e., differential pyramidality at nitrogen is apparently not a factor in the observed difference in conformational preference.[2]

It is evident from a consideration of the MM2(87) optimized equilibrium conformations of **DEAP** and **DBAP** that the site anti to the lone pair is more sterically crowded that the site gauche to the lone pair. In the **AGA** or **GAA** conformation, the anti methyl or phenyl group is *syn* to the methine proton and to an anti methylene proton. Using the *A* value as a measure of the steric requirements of a substituent,[29] the phenyl group (A = 2.9 kcal/mol)[30] is sterically larger than methyl (A = 1.7 kcal/mol).[31] The larger phenyl group will show less preference for the more crowded site anti to the lone pair than the smaller methyl moiety. Indeed, in **DBAP**, the strongly preferred enantiomeric conformations have an isopropyl methyl anti to the lone pair and both phenyl groups gauche to the lone pair. The molecular mechanics calculations also suggest a torsion of the phenyl groups in the **G'GG** and **GG'G'** conformations of **DBAP** toward the lone pair. In the **G'GG** form of **DBAP**, dihedral angles C2−N1−C7−C8 and C2−N1−C5−C6 are −168° and 57.9°, respectively. The larger phenyl group moves toward the sterically unencumbered region proximate to the lone pair. The corresponding dihedral angles in **DEAP** are −173.3° and 52.2° indicating a smaller torsion of the methyl groups toward the lone pair that is consistent with a sterically smaller methyl group.

(29) Bushweller, C. H. In *Conformational Behavior of Six-Membered Rings. Analysis, Dynamics, and Stereoelectron Effects*; Juaristi, E., Ed.; VCH Publishers: New York, 1995.

(30) Eliel, E. L.; Manoharan, M. *J. Org. Chem.* **1981**, *46*, 1959.

(31) Anet, F. A. L.; Bradley, C. H.; Buchanan, G. W. *J. Am. Chem. Soc.* **1971**, *93*, 258. Booth, H.; Everett, J. R. *J. Chem. Soc., Perkin Trans. 2* **1980**, 255.

Experimental Section

NMR Spectra. The NMR spectra were recorded by using a Bruker WM-250 NMR system at the University of Vermont and a Bruker WP-270 NMR system at the Northwest Regional NMR Facility at Yale University. The WM-250 magnet pole gap was modified to allow safe operation (no magnet O-ring freezing) down to 93 K. NMR sample temperature was varied by using a custom-built cold nitrogen gas delivery system used in conjunction with the Bruker BVT-1000 temperature control unit. Temperature measurement is accurate to ±3 K. NMR samples were prepared in precision 5- or 10-mm tubes and sealed after 4 freeze−pump−thaw cycles. All spectra are referenced to tetramethylsilane at 0 ppm.

2-(Diethylamino)propane (DEAP). 2-Aminopropane (12 g, 0.2 mol) was placed in a 3-neck round-bottom flask fitted with an efficient condenser equipped with a drying tube. With stirring and cooling, a solution of acetyl chloride (18 g, 0.1 mol) in ether (50 mL) was added dropwise. The mixture was stirred at room temperature for 24 h. With cooling and stirring, an aqueous 35% NaOH solution (45 g) was added dropwise. The mixture was stirred at room temperature for 2 h. The ether layer was extracted. The bulk of the ether and excess amine were removed first by careful distillation and then under vacuum to leave a clear liquid. Pure 2-propylacetamide was confirmed by ^{1}H NMR. 2-Propylacetamide (4 g, 0.04 mol) in anhydrous ether (80 mL) was placed in a 3-neck round-bottom flask fitted with an efficient condenser equipped with a drying tube. With cooling and stirring, 1 M ethereal $LiAlH_4$ (50 mL, 0.05 mol) was added dropwise. The mixture was refluxed for 5 h. With cooling and stirring, an aqueous 10% NaOH solution (20 g) was added. The resulting mixture was filtered, and the ether layer was extracted and dried over anhydrous Na_2SO_4 for 12 h. 2-(Ethylamino)propane in ether was confirmed by ^{1}H NMR. The dried amine solution was placed in a 3-neck round-bottom flask fitted with an efficient condenser equipped with a drying tube. With cooling and stirring, a solution of acetyl chloride (4 g, 0.051 mol) in ether (50 mL) was added dropwise. The mixture was stirred at room temperature for 24 h. With cooling and stirring, solid NaOH (20 g) was slowly added. The mixture was gravity filtered. The ether and excess amine were removed under vacuum to yield a yellow oil. *N*-Ethyl-2-propylacetamide was confirmed by ^{1}H NMR. *N*-Ethyl-2-propylacetamide (2 g, 0.015 mol) in ether (40 mL) was dried over anhydrous Na_2SO_4 for 12 h. The solution was filtered and placed in a 3-neck round-bottom flask fitted with an efficient condenser equipped with a drying tube. With cooling and stirring, 1 M ethereal $LiAlH_4$ (16 mL, 0.016 mol) was added dropwise. The mixture was refluxed for 5 h and cooled, and an aqueous 10% NaOH solution (10 g) was added dropwise. The resulting mixture was filtered, and the ether layer was extracted and dried over anhydrous Na_2SO_4 for 12 h. The bulk of the ether was removed by careful distillation under 1 atm of nitrogen. 2-(Diethylamino)propane (**DEAP**) was purified on a 25% SF-96/5% XE-60 on Chromosorb WAW GLC column (20 ft × $^3/_8$ in.) at 373 K. Characterization was done by mass spectroscopy *m/e* (M^+) 115, ^{13}C NMR (see text), and ^{1}H NMR (250 MHz; 3% v/v in $CBrF_3$ at 190 K): doublet (δ 0.98; $^3J_{HCCH}$ = 6.3 Hz; $C(CH_3)_2$), a triplet (δ 1.04; $^3J_{HCCH}$ = 7.3 Hz; $2(CCH_3)$), a quartet (δ 2.45; $^3J_{HCCH}$ = 7.3 Hz; $2(CH_2)$), a septet (δ 2.94; $^3J_{HCCH}$ = 6.3 Hz; CH).

2-(Diethyl-*2,2,2-d*$_3$)amino)propane-*2-d* [$(CH_3)_2CDN(CH_2CD_3)_2$; DEAP-d_7]. To a cooled (280 K) stirred solution of 4.5 g (0.046 mol) of 2-aminopropyl-*2-d* hydrochloride (prepared as described previously[19]) in 20 mL of water and 30 mL of diethyl ether was added slowly 2.6 g (0.046 mol) of KOH in 5 mL of water. The ether and water layers were separated. A 15-g sample of ethyl-*2,2,2-d*$_3$ iodide (MSD Isotopes) was added slowly to the ether solution containing 2-aminopropane-*2-d*. The reaction mixture was allowed to reflux for 2 h and 15 mL of water was added. The aqueous layer was then saturated with KOH. The ether and water layers were separated. The ether solution was dried over anhydrous Na_2SO_4 and filtered, and the ether was removed by careful distillation on a spinning band column. 2-(Diethyl-*2,2,2-d*$_3$-amino)propane-*2-d* was purified on a 20% SE-30 GLPC column. $^1H\{^2H\}$ NMR ($CBrF_3$; 200 K): δ 0.99 (6H, singlet, $CD(CH_3)_2$), δ 2.42 (4H, singlet, CH_2CD_3).

2-(Dibenzylamino)propane (DBAP). Isopropylamine (12 g, 0.203 mol) in ether (100 mL) was placed in a round-bottom flask fitted with

an efficient condenser equipped with a drying tube. With cooling and stirring, benzoyl bromide (19 g, 0.010 mol) was added dropwise resulting in a white precipitate. The reaction mixture was stirred at room temperature for an additional 12 h. With cooling and stirring, solid KOH (20 g) was added. The mixture was stirred at room temperature for 5 h and filtered, and the ether and excess amine were removed under vacuum to yield a white solid (mp 96−98 °C). Isopropylbenzamide was confirmed by ^{1}H NMR. Isopropylbenzamide (6 g, 0.037 mol) in ether (50 mL) was placed in a 3-neck round-bottom flask fitted with an efficient condenser equipped with a drying tube. With cooling and stirring, 1 M ethereal $LiAlH_4$ (40 mL, 0.04 mol) was added dropwise. The mixture was refluxed for 5 h. With cooling and stirring, an aqueous 15% NaOH solution (20 mL) was added to the reaction mixture. The mixture was filtered and the ether layer was extracted and dried over Na_2SO_4 for 2 h. Isopropylbenzylamine in ether was confirmed by ^{1}H NMR. The ether solution was placed in a 3-neck round-bottom flask fitted with an efficient condenser equipped with a drying tube. With cooling and stirring, benzoyl bromide (7 g, 0.038 mol) was added dropwise. The mixture was refluxed for 6 h. With cooling and stirring, solid KOH (20 g) was slowly added. The mixture was stirred at room temperature for 12 h and filtered, and the bulk of the ether and excess amine were removed by rotary evaporation to yield a yellow oil. ^{1}H NMR confirmed crude benzylisopropylbenzamide contaminated with less than 1% isopropylbenzylamine. An attempt at vacuum distillation of a portion of the oil resulted in decomposition. Crude isopropylbenzylbenzamide (8.7 g) in ether (30 mL) was dried over Na_2SO_4 for 12 h. The solution was filtered and placed in a 3-neck round-bottom flask fitted with an efficient condenser equipped with a drying tube. With cooling and stirring, 1 M ethereal $LiAlH_4$ (70 mL, 0.07 mol) was added dropwise. The mixture was refluxed for 5 h. With cooling and stirring, an aqueous 5% NaOH solution (20 mL) was slowly added. The resulting mixture was vacuum filtered. The bulk of the ether was removed by rotary evaporation. 2-(Dibenzylamino)propane was purified by careful vacuum distillation (bp 120 °C at 1 mm). 2-(Dibenzylamino)propane was confirmed by ^{1}H NMR (see text), ^{13}C NMR (see text), and mass spectroscopy *m/e* (M^+) 239.

Acknowledgment. C.H.B. is grateful to the National Science Foundation (Grant No. CHE80-24931) and to the University of Vermont Committee on Research and Scholarship for partial support of this research.

JA9531539